ELSEVIER

Thermochimica Acta 304/305 (1997) 35–49

thermochimica acta

Ultrasonic relaxation and complex heat capacity

Ingo Alig

Deutsches Kunststoff-Institut, Schloßgartenstraße 6, D-64289 Darmstadt, Germany

Received 11 September 1996; accepted 4 April 1997

Abstract

The similar origin of the sound absorption due to thermal relaxation processes in ultrasonic experiments and the frequency-dependent complex heat capacity measured by temperature-modulated calorimetric (TMC) experiments is reviewed. Furthermore, the similarities and limitations of the two experimental methods for investigations of the glass relaxation and the relaxation of composition fluctuations near a second-order critical point are discussed. The theories for the ultrasonic attenuation near a second-order phase transition, which include the description of the complex frequency-dependent heat capacity, are referred to and illustrated with some examples. It has been shown that, for those relaxation processes the ultrasonic spectroscopy can be considered as a high-frequency extension of the TMC. © 1997 Elsevier Science B.V.

Keywords: Ultrasonic; Heat capacity; Temperature-modulated calorimetric

1. Introduction

With the application of temperature modulation to a differential scanning calorimeter (DSC) by Reading et al. [1–4] a considerable progress in classical thermal analysis has been triggered. As Wunderlich et al. [5] noticed recently, this may well be called the greatest advance in scanning calorimetry since its inception thirty-five years ago. Parallel to the development of modulated differential scanning calorimeters (MDSC) a discussion about the physical meaning of the additional information provided by this technique started. This discussion was mainly stimulated by Schawe [6–8] who interpreted the temperature-modulated DSC (TMDSC) measurements in terms of a complex heat capacity.

Some years before the development of the TMDSC equipment, Nagel et al. [9,10] introduced specific-heat spectroscopy using periodic electrical heating of the sample and the analysis of the first and the third harmonic responses for calculation of the frequency-dependent heat capacity.

The fact that Nagel et al. compared the relaxation times estimated from their specific-heat spectroscopy to ultrasonic relaxation data is, from a physical point of view, very reasonable, as shown below, but may have been rather arbitrary in this paper [11].

A careful analysis of the literature by Gmelin [12] shows that modulated sample heating using different forms of energy (resistive or inductive, Joule heating, light, electron bombardment, etc.) is common in calorimetry since 1911 [13]. Therefore, we can consider the temperature-modulated calorimetry (TMC) as a rather classical method. At this point, one may recall that the thermal waves were already investigated by Fourier [14] at the beginning of the last century and have been applied by Angström [15] for measurements of thermal conductivity. The so-called thermal

PII S0040-6031(97)00174-3

wave imaging, which is based on temperature modulations on the surface of a sample and the differences in the thermal diffusion length (a combination of thermal conductivity, heat capacity and density) at different positions of a material, is applied for non-destructive evaluation [16] of large objects or for microscopic imaging (see, e.g. [17]). Similar to the complex heat-capacity measurements discussed here, both, phase and amplitude, can be used for the imaging.

If one is interested in a better molecular description of the frequency-dependent heat capacity, one will find that many of the ideas have been developed in order to understand the attenuation of sound. As early as 1816, Laplace [18] demonstrated that the velocity of sound is associated with adiabatic rather than isothermal compressibility. Therefore, during propagation of a sound wave, the oscillation of acoustic pressure is coupled with adiabatic temperature oscillations. The latter is very similar to a temperature-modulated calorimetric experiment. Hence, adiabatic temperature oscillations are of importance for the understanding of sound attenuation, as shown in 1928 by Herzfeld and Rice [19] for polyatomic gases. They noted that the transfer of energy from external degrees of freedom (i.e. the translational degrees of freedom of gases) to the internal degrees of freedom (i.e. the vibrational modes of oscillation and rotational modes in polyatomic gases) is characterised by one or a series of characteristic relaxation times τ_i. In the case of sound frequency ω (angular frequency – $\omega = 2\pi f$), which is identical to the frequency of the temperature modulation, being less than the inverse of the relaxation time τ_i, the internal and external degrees of freedom are in equilibrium. If, on the other hand, ω is much faster than the inverse of τ_i, the internal degrees of freedom cannot follow the external ones. For ω equal to $1/\tau_i$, the internal modes show a maximum phase shift compared to external ones, i.e. to the external temperature. The resulting dispersion can then be described by a complex frequency-dependent heat capacity. For a description of sound propagation, the complex frequency-dependent heat capacity can be connected to a complex compressibility and, furthermore, to a complex sound velocity [20]. It can be shown that sound attenuation is related to the imaginary part of the complex heat capacity and reflects the frequency dependence of energy transfer between internal and external degrees of freedom. A first theory for the anomalous absorption of sound near a second-order phase transition was developed by Landau and Khalatnikov [21] according to the formalism for the relaxation phenomena developed by Mandelstam and Leontovich [22]. They [21] showed that the amplitude of the sound absorption can be expressed by the specific heat at a second-order phase transition. Later, Fixman [23] and Mistura [24] applied the Herzfeld–Rice idea to second-order phase transitions. These theories for longitudinal ultrasonic attenuation include the expressions for a complex frequency-dependent heat capacity near a critical point. In 1985, Ferrell and Bhattacharjee [25] extended the Herzfeld–Rice–Fixman–Mistura approach by adding the idea of dynamical scaling. This theory proved to be rather successful for the description of ultrasonic attenuation data near a second-order phase transition, as shown by several ultrasonic investigations (see e.g. Refs. [26–29] and references therein).

The aim of this paper is to review some of the theories for the frequency-dependent heat capacity which have been developed for a description of sound attenuation. The relationship between the complex frequency-dependent heat capacity measured by calorimetric and ultrasonic experiments may stimulate the ongoing discussion on temperature-modulated calorimetry. It will be shown that ultrasonic experiments, in some sense, may be considered as a high-frequency extension of the TMC. The formal similarities between TMC and other relaxation techniques are discussed.

2. Complex heat capacity

2.1. *Energy transfer from external to internal degrees of freedom*

Relaxation phenomena (for details, see Ref. [20]) are usually described by linear differential equations, in which only the first and the zeroth differential quotients are taken into account. For example, in contrast to the second-order linear differential equation for mechanical resonance phenomena, in the differential equation for a relaxation the inertial force is neglected and only the frictional and the restoring

forces are considered. In the case of an external field, the resulting additional force has also to be taken in consideration.

Mandelstam and Leontovich [22], and most extensively Meixner [30], have shown that this type of differential equation can be derived for relaxation phenomena in a very general formalism, which does not specify the molecular mechanisms in detail. For the dependent variable an order parameter is used in this approach, which is defined with respect to the 'driving force' of the process.

As early as in 1928, Herzfeld and Rice [19] assumed that, for the explanation of the sound attenuation in polyatomic gases, the transfer of energy from external degrees of freedom to the internal degrees of freedom can be expressed by a typical relaxation equation containing a characteristic relaxation time τ for the energy exchange between external and internal degrees of freedom:

$$-\frac{dE^i}{dt} = \frac{1}{\tau}\left[E^i - E^i(T^e)\right], \tag{1}$$

where E^i is the momentary value of the internal energy and $E^i(T^e)$ the value it would have in equilibrium with the external degrees of freedom. The latter are represented by the temperature T^e.

When assuming that the heat capacity C^i is independent of the temperature or that the deviations of the temperature from a value T_0 are small, one can write

$$E^i - E^i_0 = C^i(T^i - T_0), \tag{2}$$

with C^i being the heat capacity due to the internal degrees of freedom, which are represented by a temperature T^i. The assumption of a temperature-independent heat capacity is quite strong since temperature changes in a sample are connected mostly to changes in the internal degrees of freedom and, therefore, to changes in the heat capacity. This limits the amplitude of the temperature modulations in the experiments to very small values. In particular, it may become very difficult to fulfill this assumption close to phase transition. A similar problem can arise from applying the temperature-modulation technique to irreversible processes or those controlled by slow diffusion (i.e. crystallisation in polymers). However, with the assumption of a temperature-independent heat capacity Eqs. (2) and (3) can rewritten as:

$$-\frac{dT^i}{dt} = \frac{1}{\tau}(T^i - T^e). \tag{3}$$

Different temperature changes (temperature steps, harmonic excitation, etc.) can now be applied to systems for which internal and external degrees of freedom are defined [20].

2.2. Step function

A typical time-domain relaxation experiment involves the excitation of the sample by a step function and recording the response. In our case, it is possible to raise, or decrease, the external temperature at $t = 0$ from T_0 to a value of T_1. Two cases may be discussed now: (i) the external temperature is kept constant at T_1 after $t = t_0$ and the energy, which is transferred to the internal degrees of freedom, replaced from the thermal bath; and (ii) the external temperature is not constant but lowered by the amount of energy transferred into the internal degrees of freedom.

In the first case, the external rise in temperature is defined by the step function

$$T^e(t) = \begin{cases} T_0 & t < t_0 \\ T_1 & t \geq t_0. \end{cases} \tag{4}$$

The solution of Eq. (4) is then given by

$$T^i(t) = T_1 + (T_0 - T_1)\exp\left(-(t - t_0)/\tau\right) \tag{5}$$

This situation is shown schematically in Fig. 1.

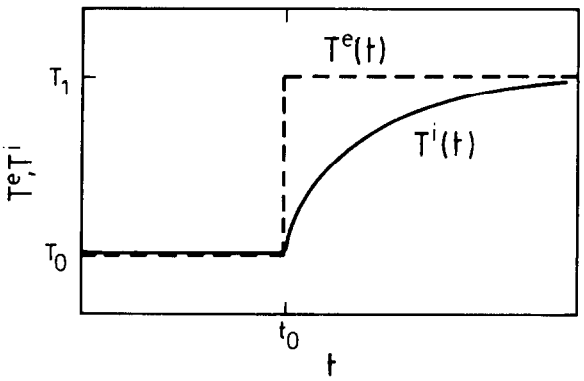

Fig. 1. Response of internal temperature (internal degrees of freedom) after a temperature step from T_0 to T_1 at $t = t_0$ (the external temperature is kept constant at T_1 for $t > t_0$).

In case of the external temperature not being constant but depending on the amount of energy flowing into internal degrees of freedom (with no energy transfer from the thermal bath to the external degrees of freedom after the temperature step), one can obtain for a rise in the external temperature from T_0 to a value T_1 at $t = t_0$ (see Ref. [20]) the following:

$$T^{\mathrm{i}}(t) = T_2 + (T_0 - T_2)\exp\{-(t - t_0)/\tau'\}, \tag{6}$$

with

$$\tau' = \frac{C - C^{\mathrm{i}}}{C}\tau, \tag{7}$$

where, in contrast to Eq. (4), T^{e} is not constant for $t > t_0$ ($T^{e} \to T_2$ as $t \to \infty$). From Eq. (7), it can be seen that the characteristic relaxation time depends on the circumstances of the experiments.

2.3. Harmonic excitation

The typical relaxation experiment to get directly the response function in the frequency domain is a harmonic excitation of the system with different frequencies. For a periodic variation of temperature with time around T_0, one can write

$$\delta T(t) \equiv \delta T^{\mathrm{e}} = T^{\mathrm{e}} - T_0 \propto \mathrm{e}^{i\omega t}. \tag{8}$$

The temperature response of the internal degrees of freedom is then defined by

$$\delta T^{\mathrm{i}} \equiv T^{\mathrm{i}} - T_0 \propto \mathrm{e}^{i(\omega t - \varphi)} \tag{9}$$

with the angular frequency ω and the phase shift φ between the temperature of external and internal degrees of freedom. The temperature response of the internal degrees of freedom can be expressed by

$$-\frac{\mathrm{d}(\delta T^{\mathrm{i}})}{\mathrm{d}t} = \frac{1}{\tau}(\delta T^{\mathrm{i}} - \delta T^{\mathrm{e}}), \tag{10}$$

which is an extension of Eq. (3). For the periodic temperature variation defined in Eq. (8), we get for the stationary state

$$\delta T^{\mathrm{i}}(t) = \frac{\delta T^{\mathrm{e}}(t)}{1 + j\omega\tau}. \tag{11}$$

The effective frequency-dependent heat capacity C_{v}^{*} at constant volume is then defined by

$$\begin{aligned} \mathrm{d}E = C_{\mathrm{v}}^{*}\delta T^{\mathrm{e}} &\equiv C_{\mathrm{v},\infty}\delta T^{\mathrm{e}} + C_{\mathrm{v}}^{\mathrm{i}}\delta T^{\mathrm{i}} \\ &= \left(C_{\mathrm{v},\infty} + C_{\mathrm{v}}^{\mathrm{i}}\frac{\delta T^{\mathrm{i}}}{\delta T^{\mathrm{e}}}\right)\delta T^{\mathrm{e}}, \end{aligned} \tag{12a}$$

with

$$C_{\mathrm{v}}^{*}(\omega) = C_{\mathrm{v},\infty} + \frac{C_{\mathrm{v}}^{\mathrm{i}}}{1 + j\omega\tau} \quad \text{and} \quad C_{\mathrm{v}}^{\mathrm{i}} = C_{\mathrm{v},o} - C_{\mathrm{v},\infty}. \tag{12b}$$

In case the internal degrees of freedom are in equilibrium with the external ones, i.e. for low frequencies of temperature variation ($\omega \to 0$), the static heat capacity $C_{\mathrm{v},0}$ can be subdivided into two parts: one belonging to the external degrees of freedom ($C_{\mathrm{v}}^{\mathrm{e}}$) and the other to the internal degrees of freedom ($C_{\mathrm{v}}^{\mathrm{i}}$). In this situation, the effective frequency-dependent heat capacity of the sample $C_{\mathrm{v}}^{*}(\omega)$ becomes identical to the static heat capacity $C_{\mathrm{v},0} = C_{\mathrm{v}}(\omega = 0) = C_{\mathrm{v}}^{\mathrm{e}} + C_{\mathrm{v}}^{\mathrm{i}}$. In case the temperature changes are much faster compared to the characteristic relaxation time τ, only the external degrees of freedom can contribute to the effective heat capacity $C_{\mathrm{v}}^{*}(\omega \to \infty) \equiv C_{\mathrm{v},\infty} = C_{\mathrm{v}}^{\mathrm{e}}$. The 'relaxation strength' in Eq. (12b) is then identical with the contribution of the internal degrees of freedom to the static heat capacity $C_{\mathrm{v}}^{\mathrm{i}} = C_{\mathrm{v},0} - C_{\mathrm{v},\infty}$.

Eqs. (12a) and (12b) define a complex frequency-dependent heat capacity, with a real part C_{v}', and an imaginary part C_{v}'', respectively.

$$C_{\mathrm{v}}^{*} \equiv C_{\mathrm{v}}' - jC_{\mathrm{v}}'' = C_{\mathrm{v},\infty} + \frac{C_{\mathrm{v}}^{\mathrm{i}}}{1 + \omega^2\tau^2} - j\frac{C_{\mathrm{v}}^{\mathrm{i}}\omega\tau}{1 + \omega^2\tau^2}. \tag{13}$$

The frequency dependence of C_{v}' and C_{v}'' is illustrated in Fig. 2a for a single relaxation time τ. In most systems, the situation is much more complicated and the single relaxation process has to be replaced by a distribution of relaxation times.

In contrast to the ultrasonic measurements in liquids [20], where the relative changes in volume are considered to be small during the relaxation, in calorimetric experiments the pressure is usually kept constant. In this case, the energy in Eqs. (12a),(12b) and (13) has to be replaced by the enthalpy and all indices in the heat capacity which do refer to a

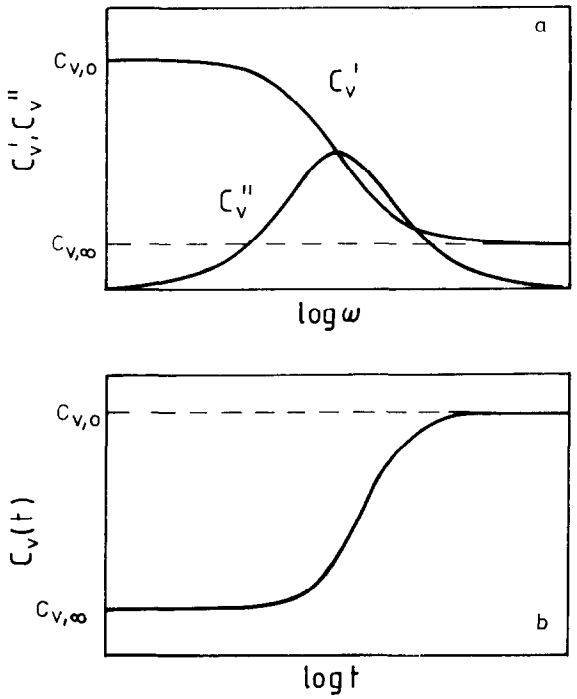

Fig. 2. (a) – Frequency dependence of the real and imaginary parts of the complex heat capacity. $C_{v,0}$ and $C_{v,\infty}$ are the limiting values of the heat capacity at low (static) and high freqencies, respectively. (b) – Heat capacity $C_v(t)$ as a function of time after an instantaneous temperature rise by ΔT at $t = 0$.

constant volume 'v' have to replaced by 'p' for constant pressure. One will notice that for many relaxation processes in condensed matter, i.e. when the changes in the internal degrees of freedom are not coupled with changes in volume, δH^i can be replaced by δE^i even in case of constant-pressure experiments [20].

2.4. Real and imaginary part of the frequency-dependent heat capacity

Since the complex heat capacity is a generalised compliance in the theory of linear response, the real and imaginary parts are connected by the Kramers–Kronig relations:

$$\Re\mathrm{e}\{C_p^*(\omega)\} = \frac{1}{\pi} P \int_{-\infty}^{+\infty} \frac{\Im\mathrm{m}\{C_p^*(\xi)\}}{\xi - \omega} \mathrm{d}\xi, \qquad (14a)$$

and

$$\Im\mathrm{m}\{C_p^*(\omega)\} = \frac{1}{\pi} P \int_{-\infty}^{+\infty} \frac{\Re\mathrm{e}\{C_p^*(\xi)\}}{\xi - \omega} \mathrm{d}\xi, \qquad (14b)$$

where P denotes the Cauchy principal value. In contrast to the dielectric or mechanical loss, the imaginary part of the heat capacity is not connected to an effective energy dissipation, and can be related via classical thermodynamics to the entropy change as follows:

$$\delta S = \pi \Im\mathrm{m}\left(C_p^*(\omega)\right) \frac{\delta T}{T} \qquad (15)$$

From the second law of thermodynamics [34], it follows that $\Im\mathrm{m}C_p^*(\omega)) \geq 0$. However, a formal similarity to the loss component of mechanical or dielectric compliance can be found, considering the energy loss of the external degrees of freedom due to the phase shift between δT^e and δT^i. In the temperature-modulation experiment, the energy of the external degrees of freedom leaks into the internal degrees of freedom, i.e. from one 'form of energy' to the other 'form of energy'. This seems quite similar to the energy loss of an external mechanical or electrical field, which is transferred into heat of the sample. In both cases, it has to be proved whether the limitations for linear systems are fulfilled (or, at least, can be approximated in the experiment) or not.

2.5. Principle of superposition

As shown in Fig. 1, the internal degrees of freedom respond to an instantaneous temperature rise ΔT^e by a time-dependent temperature change, which is an exponential function in the simplest case (see Eq. (5)). With $\Delta H(t) = C_p(t)\Delta T^e$ one can formally define [31] a time-dependent heat capacity $C_p(t)$ for the temperature step excitation. For example, a schematic representation of $C_v(t)$ as a function of time after an instantaneous temperature rise ΔT at $t = 0$ is shown in Fig. 2b.

Based on the assumption of linear superposition of the enthalpy response (for an illustration, see Fig. 3) after a series of temperature steps $\Delta T_k(t_k)$ one can write, using a time-dependent heat capacity $C_p(t)$,

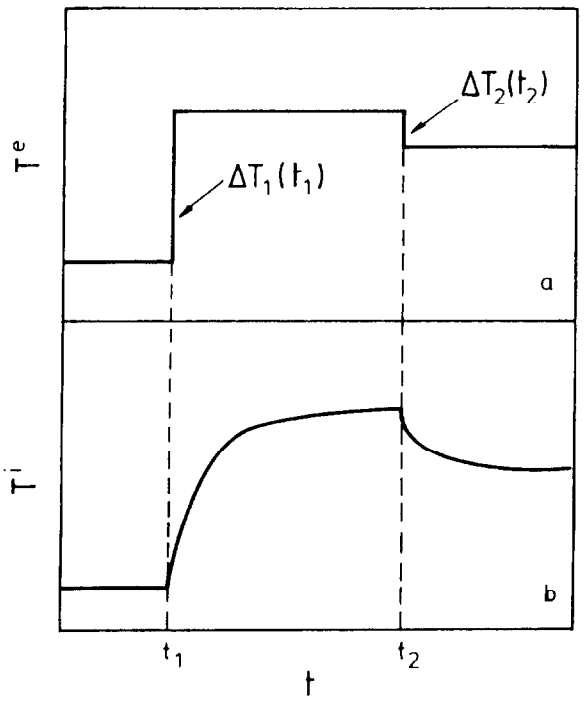

Fig. 3. Schematic representation of (b) – the temperature response of the internal degrees of freedom after a series of (a) – external temperature steps ΔT_k at times t_k . The external temperature is kept constant in the intervals between t_k and t_{k+1}. Only two temperature steps at t_1 and t_2 are shown.

$$\Delta H(t) \equiv \sum_k \Delta H_k(t-t_k) = \sum_k C_p(t-t_k)\Delta T_k(t_k). \tag{16}$$

If we go to the integral representation [31], with a normalised response function $\Phi(t)$, we get

$$\Delta H(t) \equiv \int_{-\infty}^{t} \left\{ C_{p,\infty} + (C_{p,0} - C_{p,\infty}) \times [1-\Phi(t-t')] \right\} \Delta\dot{T}(t')\mathrm{d}t' = C_{p,\infty}\Delta T(t) - \int_0^{\infty} \{(C_{p,0}-C_{p,\infty})\dot{\Phi}(\zeta)\}\Delta T(t-\zeta)\mathrm{d}\zeta, \tag{17}$$

with $\zeta = t - t'$ and the 'relaxation strength' $\Delta C_p = C_{p,0} - C_{p,\infty}$ which may be considered as the phonon contribution in the case of condensed matter or the contribution from translational degrees of freedom for a polyatomic gas. The response in the enthalpy change after a temperature step ΔT at $t = 0$ is then given by:

$$\Delta H(t) = \begin{cases} 0 & \text{for } t<0 \\ \{C_{p,\infty} + (C_{p,0} - C_{p,\infty})[1-\Phi(t)]\}\Delta T & \text{for } t>0 \end{cases} \tag{18}$$

It can be seen that the term in the curly brackets in Eq. (18) is the time-dependent heat capacity $C_p(t)$.

For a harmonic excitation $\Delta T \propto \delta T^e \propto e^{i\omega t}$, hence one gets from Fourier transformation in the frequency domain the following:

$$\Delta H(\omega) = C_p^*(\omega)\Delta T(\omega) \text{ or}$$
$$\delta H(\omega) = C_p^*(\omega)\delta T^e(\omega), \tag{19}$$

with

$$C_p^*(\omega) = C_{p,\infty} - (C_{p,0} - C_{p,\infty}) \int_0^{\infty} [-\dot{\Phi}(t)]e^{j\omega t}\mathrm{d}t. \tag{20}$$

For the assumption that the normalised response function $\Phi(t)$ is a single exponential decay, Eq. (20) has the same structure as Eqs. (12a) and (12b). For more complex relaxation processes $\Phi(t)$ can be expressed by a superposition of exponential functions or a Kohlrausch law [32] $\Phi(t) = \exp(-(t/\tau)^{\beta})$ (with $0 < \beta \leq 1$).

The structure of Eq. (20) is identical to the equations in the more generalised description of the linear response theory. In this approach, the frequency-dependent heat capacity can be considered as generalised susceptibility. Therefore, it is reasonable to compare the susceptibilities for different external excitations. This has been done recently by Hensel et al. for temperature-dependent TMDSC and dielectric relaxation measurement on poly(vinyl acetate) in the glass-transition region [8]. In Fig. 4 the temperature dependence of the real (c_p') and the imaginary part (c_p'') of the complex specific heat capacity ($f = 0.04$Hz, $q = -1.12$K/min) is shown together with that of the real (ε') and imaginary part (ε'') of the dielectric function ($f = 1$kHz, $q = 0.5$K/min). The total c_p, which is almost identical to $c_{p,0}$ and

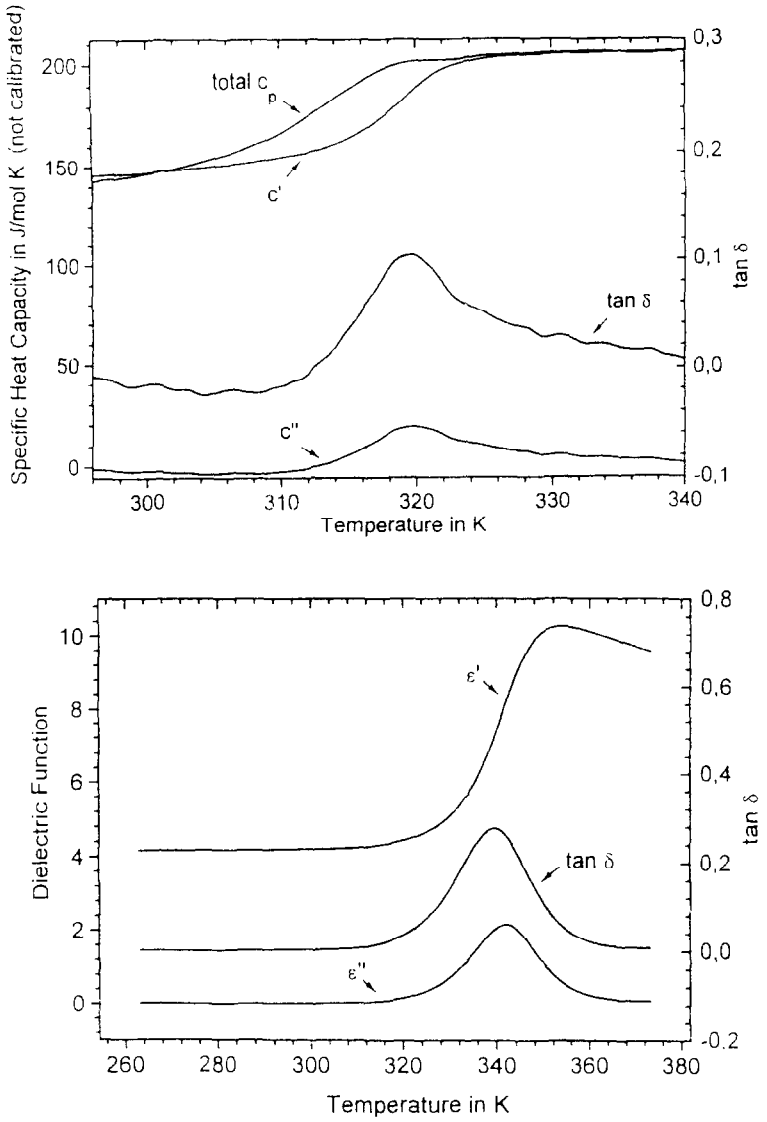

Fig. 4. (a) Temerature dependence of the real (c'_p) and imaginary part (c''_p) of the complex specific heat capacity for poly (vinyl acetate) in the glass transition region (f=0.04 Hz, q=−1.12 K/min) [8]. tan$\delta = c''_p/c'_p$ is the loss tangent. The total cp "can be identified by $c_{p,0}$ in the text. (b) temperature dependence of the real (ε') and imaginary part (ε'') of the dielectric function in the glass transition region of poly(vinyl acetate) (f=1k Hz, q=0.5K/min)[8]. The loss tangent is tan $\delta = \varepsilon''/\varepsilon'$.

the loss tangents tan$\delta = c''_p/c'_p$ and tan$\delta = \varepsilon''/\varepsilon'$ for the TMDSC and dielectric experiment, respectively, are also presented.

Hensel et al. have shown (see Fig. 5) by extrapolation of the Vogel–Fulcher equation [33] ($\tau = \tau_0 \exp[B/(T - T_0)]$, where T_0 is the Vogel temperature and B and τ_0 parameters) for the relaxation times from dielectric experiments to the frequency range of TMDSC, that there is, at least in principle, an agreement in the temperature dependence of the relaxation times of the two methods for the dynamic glass transition [35–37].

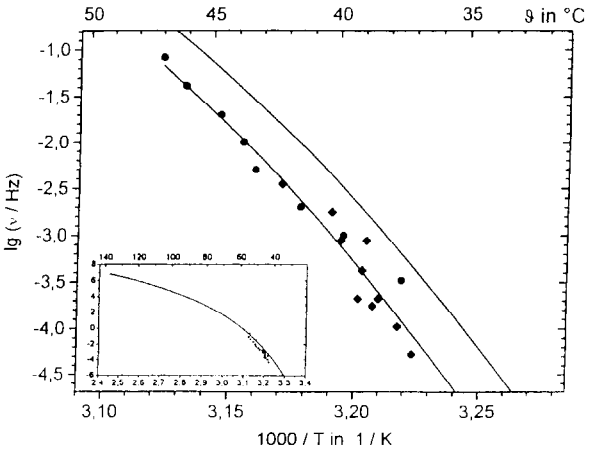

Fig. 5. Activation plot for poly(vinyl acetate) from reference [8]. The temperatures are taken from the maximum in c_p''(●), the glass transition temperature from standard DSC (◆) (the transformation of the cooling rate into a frequency is described in [8]), and the maximum in the imaginary part (ε'') of the dielectric function (x). The inset shows the frequency range of dielectric experiments. The lines represent a fit with Vogel–Fulcher equation (for the parameters, see [8]).

2.6. Enthalpy fluctuations and heat capacity

From statistical thermodynamics [34], it is known that the static heat capacity can be related to the fluctuations of entropy at equilibrium, which are identical to the fluctuations of enthalpy at constant pressure

$$C_{p,0} = \frac{V}{k_B T^2} \langle (\delta H)^2 \rangle. \tag{21}$$

with the volume V, the Boltzmann constant k_B and $\delta H(t) = H(t) - \langle H \rangle$. The brackets indicate the thermodynamic average, where $\langle H \rangle$ is the average of $H(t)$.

Using the fluctuation–dissipation theorem, a static susceptibility can be related to a time-dependent correlation function, which can be extended to the dynamic susceptibility. In the fluctuation picture, the response of a system to an external perturbation is considered to have the same dynamics as the decay of spontaneous fluctuations. The normalised response function in Eqs. (17),(18) and (20) can then be related to the auto-correlation function of enthalpy

$$\Phi(t) = \frac{\langle \delta H(t) \delta H(0) \rangle}{\langle (\delta H)^2 \rangle}. \tag{22}$$

For the complex frequency-dependent heat capacity, it follows:

$$C_p^*(\omega) = C_{p,\infty} + \left(1 - \frac{C_{p,\infty}}{C_{p,0}}\right) \frac{V}{k_B T^2} \cdot \int_0^\infty \left[-\frac{d}{dt} \langle \delta H(t) \delta H(0) \rangle \right] e^{i\omega t} dt. \tag{23}$$

3. Propagation of ultrasound and frequency-dependent heat capacity

3.1. Sound velocity and attenuation

In a classical fluid, a propagating sound wave is attenuated by the mechanism of viscous damping α_{vis} and heat conduction α_{cond}. The classical absorption coefficient α_{class} (length^{-1}) behaves like $\alpha_{class} \propto f^2$ (Kirchhoff–Stokes law, see, e.g. [38]), where f is the frequency. α_{class} [20] can be expressed by

$$\alpha_{class} = \frac{2\pi^2 f^2}{\rho u^3} \left[\left(\eta_v + \frac{4}{3} \eta_s \right) + \Lambda \left(c_v^{-1} - c_p^{-1} \right) \right], \tag{24}$$

where u is the velocity of sound, ρ the density, η_v and η_s the bulk and shear viscosities, c_v and c_p the specific heat capacities (per gram) at constant volume and pressure, respectively, and Λ the coefficient of heat conductivity. The first term in Eq. (24) refers to viscous damping α_{vis} and the second term to damping by heat conduction α_{cond}, where in liquids the heat conductivity term is small and, hence, usually neglected. Since $\alpha_{class} \propto f^2$, the ultrasonic data are often plotted as α/f^2 vs. f. In this representation, α_{class} is a straight line and relaxation processes can be well identified.

In more complex systems, e.g. polymers or systems with different phases, other processes can contribute to the observed ultrasound attenuation. Usually, the approximation is made that the contributions from relaxation α_{rel}, classical viscosity α_{vis}, heat conductivity α_{cond}, and sound scattering for inhomogeneous systems α_{sc} add up to the attenuation of sound. The sound-scattering contribution can be neglected for the glass-forming liquids and the binary mixtures considered in the following. To compare with temperature-modulated calorimetry, we will concentrate

on the relaxation contribution to the ultrasonic absorption.

The relaxation contribution due to the isotropic dilatation of the sample by the longitudinal ultrasonic waves can be formally introduced into the hydrodynamic equations by a frequency-, temperature- and pressure-dependent 'bulk viscosity' $\eta_v'(\omega)$. However, the shear viscosity also has a frequency dependence for fluids with molecular relaxation processes. The shear relaxation is typical for viscoelastic systems (e.g. polymers, see [39] and references therein) and will not be discussed here in detail.

The relaxation processes, which can be formally described by a 'bulk viscosity', originate either from temperature changes, volume changes or both.

Absorption processes due to the lagged energy exchange between external and internal degrees of freedom ('Kneser' relaxations [20]) can be discussed in terms of a frequency-dependent heat capacity. Since the internal degrees of freedom are almost insensitive to changes of volume, the transitions between the different internal stages are mainly effected by temperature changes. In contrast, the so-called structural relaxation is assumed to be only originating from volume changes (with $\Delta H \cong 0$ or $\Delta C_p \cong 0$). In general, structural transition can be induced by both volume and temperature changes.

Typical thermal relaxation processes ($\Delta V \cong 0$) are the energy exchange between translation and vibrational degrees of freedom, the changes between rotational isometric forms or those due to chemical relaxations without changes in volume, which can be expressed by a complex heat capacity. The lagged response of the order-parameter fluctuation to the temperature and pressure changes in the sound wave near a critical point, which also belongs to this class, will be discussed in more detail. For the relaxation related to the dynamic glass transition, a complex coupling between structural and thermal relaxation has to be considered.

From the wave equation for the acoustic pressure propagating in a medium with loss, a complex sound velocity $u^*(\omega)$ can be defined by

$$\frac{1}{u^*(\omega)} \equiv \frac{1}{u(\omega)} - j\frac{\alpha(\omega)}{\omega} = \frac{1}{u}\left[1 - j\frac{\alpha\lambda(\omega)}{2\pi}\right], \tag{25}$$

where u is the phase velocity and α the ultrasonic absorption coefficient. In several cases, the absorption per wavelength $\alpha_\lambda = \alpha\lambda$ is used.

Assuming a system where the equation of state only depends on the temperature of the external degrees of freedom T^e only, and having a slow energy exchange between external and internal degrees expressed by a characteristic relaxation time τ, one gets

$$\left(\frac{u_0}{u} - \frac{j\alpha u_0}{\omega}\right)^2 = \frac{C_p}{C_v}\left(C_{v,\infty} + \frac{C_v^i}{1+j\omega\tau}\right) \cdot \left(C_{p,\infty} + \frac{C_p^i}{1+j\omega\tau}\right)^{-1}. \tag{26}$$

The terms in the brackets on the right-hand side are the effective frequency-dependent heat capacity at constant volume C_v^* and at constant pressure C_p^* (see, e.g. Eq. (12a)). As shown in Eqs. (20) and (23), both can be expressed in a more general form for complex relaxation behaviour. Assuming that the enthalpy change of the internal degrees of freedom is independent of pressure for a constant temperature [20], C_v^i and C_p^i can be replaced by C^i.

Separating real and imaginary parts and assuming that $v_0 \leq v$ and $\alpha(v/\omega) < 1$ in Eq. (26), the ultrasonic velocity and absorption can be approximated [20] by the following

$$\left(\frac{u_0}{u}\right)^2 = 1 - \frac{(C_p - C_v)C^i}{C_v(C_p - C^i)} \cdot \frac{\omega^2\tau'^2}{1+\omega^2\tau'^2} \tag{27}$$

$$\alpha'\lambda\left(\frac{u_0}{u}\right)^2 = \pi\frac{(C_p - C_v)C^i}{C_v(C_p - C^i)} \cdot \frac{\omega\tau'}{1+\omega^2\tau'^2}, \tag{28}$$

where $\tau' = \left[(C_p - C^i)/C_p\right]\tau$ and α' is the nonclassical absorption. With $\mu = \mu_0$ and $\tau = \tau'$, one can show that the attenuation per wavelength α_λ is proportional to the imaginary part of the complex heat capacity:

$$\alpha_\lambda \propto \Im\mathrm{m}\left\{C_p^*(\omega)\right\}. \tag{29}$$

For a relaxation process, the quantity $\alpha_\lambda = \alpha\lambda$ shows a loss maximum vs. frequency, which is similar to the imaginary part of the dielectric function for a dipole relaxation. This is schematically represented for a single relaxation process in Fig. 6.

In the following example, we will show that even for the structural relaxation connected to the glass transition where the longitudinal sound wave couples

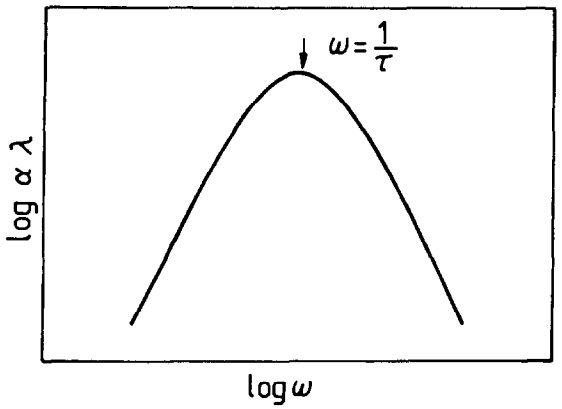

Fig. 6. Schematic representation of the loss maximum of the attenuation per wavelength $\alpha\lambda$ as a function of frequency ω. The characteristic relaxation frequency is indicated by an arrow.

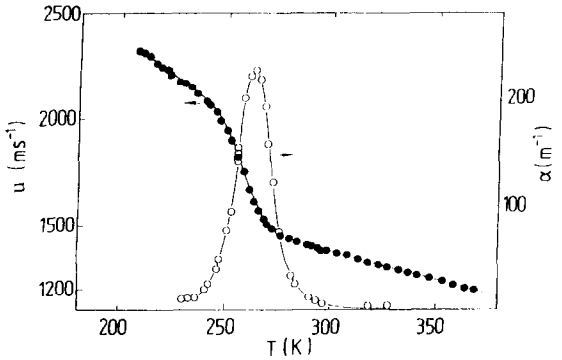

Fig. 7. Temperature dependence of the ultrasonic velocity v and the attenuation α for poly(phenylmethyl siloxane) in the glass-transition region ($f = 1$MHz) [40].

via temperature and pressure variations as well as by shear deformation with the molecular rearrangements, the similarity between ultrasonic studies and modulated calorimetry is present. In Fig. 7, the temperature dependence of the ultrasonic velocity u and attenuation α for poly(phenyl methyl siloxane) in the glass-transition region ($f = 1$MHz, $M_w = 4100$g/mol) [40] is plotted. The sound absorption shows the typical loss maximum and the sound velocity decreases with temperature in the glass-transition region. The curves are very similar to those found for c_p^* from TMDSC in PVAc (Fig. 5). Although the main characteristics of the ultrasonic attenuation resemble those of the imaginary part of the heat capacity, the temperature dependences of u and α do not originate from c_p^* alone. It is known that, in the glass-transition region, the contributions from shear excitation and volume relaxation have to be taken into consideration for longitudinal sound propagation. However, the different relaxation mechanisms seem to be strongly coupled in the glass-transition region, thus leading to the similar shapes of the temperature or frequency dependences. Parallel longitudinal and shear-wave ultrasonic investigations, together with specific-heat spectroscopy in the same temperature and frequency ranges, should be helpful for a better understanding of coupling of different modes in the glass-transition region.

3.2. *Complex heat capacity and sound parameters near a second-order phase transition*

The ultrasonic behavior of critical fluids attracted considerable attention, both experimentally and theoretically ([23–29], and [41–48]). The experimental data are explained by the coupling of the sound wave with a critical-order parameter fluctuations. In binary mixtures, the following mechanism of ultrasound attenuation is widely accepted: moreover, because of adiabatic compression and expansion of the fluid in the sound wave, the local temperature and the pressure-dependent critical temperature will change. Due to the lagged response of the concentration fluctuations to this perturbations, energy is dissipated.

The time scale of the decay of critical-concentration fluctuations is characterized by a frequency $\omega_c \equiv 1/\tau_c = 2D/\xi^2$, where $\xi = \xi_0\varepsilon^{-\tilde{\nu}}$ is the correlation length of the critical-concentration fluctuations ($\varepsilon = (T - T_c)/T_c$ – the reduced temperature; ξ_0 – the critical amplitude; and $\tilde{\nu}$ – the critical exponent) and $D = D_0\varepsilon^{-\nu^*}$ is the mutual diffusion coefficient (ν^* – the critical exponent and D_0 –the critical amplitude). The critical dynamics of binary mixtures is then characterized by $\omega_c = \omega_0\varepsilon^{-\tilde{z}\tilde{\nu}}$, where ω_0 is the critical amplitude and $\tilde{z}\tilde{\nu}$ the critical exponent ($\tilde{z} = 3 + \tilde{x}_\eta$; and $\tilde{x}_\eta$ the critical exponent of the shear viscosity).

Experimental values of ω_0 for low molecular components and for polymers are found in the interval (1–50) GHz [42].

At low sound frequencies ($\omega\tau_c \ll 1$), the fluctuations are in equilibrium with the external pressure and

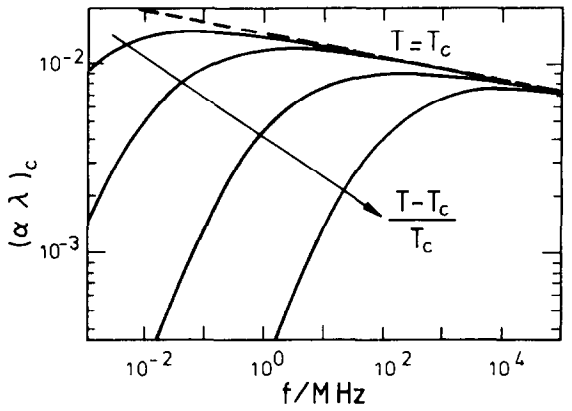

Fig. 8. Schematic representation of the critical slowing down of the ultrasonic relaxation due to critical-composition fluctuations in a binary mixture. $(\alpha\lambda)_c$ is the critical sound attenuation as a function of frequency for different values of $(T-T_c)/T_c$. The curves are calculated using the Ferrell–Bhattacharjee theory and the parameters with an aniline/cyclohexane mixture of critical composition [28] (left curve – $T - T_c = 0.05$K, right curve – $T - T_c = 30$K, $T_c = 29.72$°C). The dashed line represents the frequency dependence of $(\alpha\lambda)_c$ at the critical point $T = T_c$.

temperature changes, whereas for $\omega\tau_c \gg 1$ the fluctuations cannot follow these changes. When ω equals $1/\tau_c$, the density or composition fluctuations exhibit a maximum phase shift of the pressure and temperature oscillations. This results in a maximum in the energy dissipation, which is expressed as a maximum in α_λ (see e.g. Fig. 6). The frequency dependence of α_λ for different values of $\varepsilon = (T - T_c)/T_c$ is shown in Fig. 8. The 'critical slowing down' of the characteristic relaxation time $\tau_c(\varepsilon)$ when approaching the critical temperature ($\varepsilon = |T - T_c|/T_c \to 0$), is reflected by the different curves. The curves are calculated using the Ferrell–Bhattacharjee theory (see below) with the parameters for a critical aniline–cyclohexane mixture [28].

Theoretical studies of critical ultrasound behavior are based on calculations of the frequency-dependent complex bulk viscosity [46–48] or the frequency-dependent complex specific heat [23–25]; only the latter are considered here. Fixman [23] and Mistura [24] applied the Herzfeld–Rice idea of a frequency-dependent heat capacity to second-order phase transitions. In this theory, the internal modes are expressed by a distribution of relaxation times for the order parameter. This gives rise to the frequency-dependent heat capacity. The short relaxations times, typical for simple liquids, are shifted into the experimentally accessible frequency range by the 'critical slowing down'.

In 1985, Ferrell and Bhattacharjee [25] extended the Herzfeld–Rice–Fixman–Mistura approach by adding the idea of 'dynamical scaling'. It was shown by several ultrasonic investigations near a critical point, that this theory is rather successful for a description of ultrasonic attenuation data (see, e.g. [26–29] and references therein). This theory was found to be especially successful for describing the experimental data in the high-frequency limit (see, e.g. [29]), where a renormalisation group approach of Kroll and Ruhland [48] gives similar results. In the following, we will concentrate on the dynamic scaling theory [25]. In the Ferrell–Bhattacharjee theory, the complex sound velocity is given by

$$u^*(\omega) = u_c + \frac{g u_c^3}{2T_c c_p^*(\omega)} \tag{30}$$

u_c is the velocity of sound at the critical temperature T_c which, in turn, depends on the frequency. The dimensionless coupling constant g is defined by

$$g = -\rho c_p \left[\left(\frac{\partial T}{\partial p}\right)_S + \frac{\partial T_c}{\partial p}\right] \tag{31}$$

where $(\partial T/\partial p)_S$ represents the adiabatic change of temperature after a change in pressure, and $\partial T_c/\partial p$ the shift of the critical temperature with pressure.The ultrasonic attenuation per wavelength is then given by

$$\alpha_\lambda(\omega) = \pi \frac{u(\omega)^2 g^2}{T_c |c_p^*(\omega)|^2} \Im\mathrm{m}\left[c_p^*(\omega)\right] \tag{32}$$

The complex specific heat $c_p^*(\omega)$ can be divided into a critical $c_{p,c}^*(\omega)$ and a non-critical background $c_{p,b}$ contribution:

$$c_p^*(\omega) = c_{p,c}^*(\omega) + c_{p,b}. \tag{33}$$

For $c'_{p,c}(\omega) \gg c''_{p,c}$, the approximation $|c_{p,c}^*(\omega)| = c'_p(\omega)$ can be used. Considering the critical contribution of the complex specific heat near a critical point $c_{p,c}^*(\omega, \varepsilon) \equiv c_{p,c}^*(\omega, \omega_c)$, one can discuss two regimes: (i) the thermodynamic (ω=0) and (ii) the critical point function ($T = T_c$) [25].

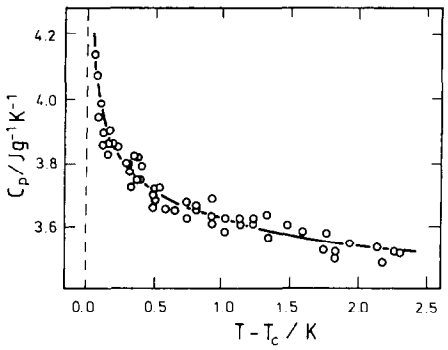

Fig. 9. Static specific heat capacity c_p of a succinonitrile/water mixture with critical compostion vs. $T - T_c$, from reference [49]. The curve represents a fit using $c_p = c_p^0 \varepsilon^{-\tilde{\alpha}} + c_{p,b}$ universal critical exponent $\tilde{\alpha} = 0.11$ (theory); system specific critical amplitude constant $c_p^0 = (0.562 \pm 0.019)\mathrm{Jg^{-1}K^{-1}}$; constant $c_{p,b} = (2.2560 \pm 0.034)\mathrm{Jg^{-1}K^{-1}}$; and critical temperature $T_c = 329.23$ K) [49].

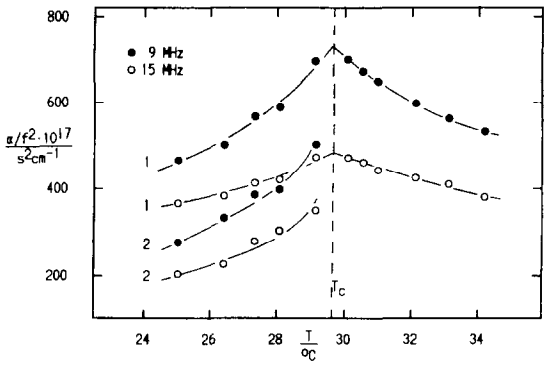

Fig. 10. Temperature dependence of the ultrasonic absorption α/f^2 for an aniline/cyclohexane mixture of critical composition [28] in the one-phase region ($T > T_c$) and the two-phase region ($T < T_c$) for frequencies of 9 MHz (filled circles) and 15 MHz (open circles). In the two-phase region the measurements have been performed in (1) – the cylcohexane-rich phase, and (2) – the aniline-rich phase.

For the thermodynamic limit (ω=0), the dynamic scaling theory yields

$$c_{p,c}(0,\omega_c) \equiv c_p^0 \left(\frac{\omega_c}{\omega_0}\right)^{-\frac{\tilde{\alpha}}{\tilde{z}\tilde{\nu}}} = c_p^0 \varepsilon^{-\tilde{\alpha}}, \tag{34}$$

with the system-specific critical amplitude of the heat capacity c_p^0 and the universal critical exponent $\tilde{\alpha} = 0.11$ (Ising theory). An experimental example for the static specific heat capacity c_p of a succinonitrile/water mixture with critical composition as a function of the reduced temperature ε is shown in Fig. 9. The data are taken from a recent publication by Knecht and Woermann [49]. The solid curves represents a fit, using for the specific heat capacity

$$c_p = c_p^0 \varepsilon^{-\tilde{\alpha}} + c_{p,b},$$

with $\tilde{\alpha} = 0.11$ (fixed).

A similar functional form is expected for the temperature dependence of the ultrasonic attenuation at a fixed frequency ($\omega > 0$):

$$\alpha_\lambda(\omega = \text{const.}, \varepsilon) \propto \Im\mathrm{m}\left[c_p^*(\omega = \text{const.}, \varepsilon)\right].$$

The ultrasonic absorption α/f^2 for an aniline/cyclohexane mixture with critical composition [28] in the one-phase ($T > T_c$) and two-phase region ($T < T_c$) are shown in Fig. 10 for frequencies of 9 and 15 MHz. In this investigation, the measurements were not only performed in the one-phase region but also in the coexisting cyclohexane-rich and aniline-rich phases. The critical contribution to the ultrasonic absorption for the two-phase region was proposed by Landau and Khalatnikov [21]. In contrast to the thermodynamic limit ($\omega = 0$) the ultrasonic attenuation and the corresponding imaginary part of the heat capacity for $\omega > 0$ do not diverge to infinity at $T = T_c$.

At the critical point ($T = T_c$), one gets for the critical part of the frequency-dependent specific heat the following:

$$c_{p,c}^*(\omega, 0) = c_p^0 \left(\frac{-i\omega}{\omega_0}\right)^{-\frac{\tilde{\alpha}}{\tilde{z}\tilde{\nu}}} \tag{35}$$

The critical exponents from the Ising theory is $\tilde{\alpha}/\tilde{z}\tilde{\nu} = 0.056$ ($\tilde{\nu} = 0.63$, $\tilde{z} = 3 + \tilde{x}_\eta$ and $\tilde{x}_\eta$=0.054). Real and imaginary parts of $c_{p,c}^*(\omega, 0)$ can be approximated by

$$c'_{p,c}(\omega, 0) \equiv \Re\mathrm{e}[c_{p,c}^*(\omega, 0)] = c_p^0 \left(\frac{\omega}{\omega_0}\right)^{-\frac{\tilde{\alpha}}{\tilde{z}\tilde{\nu}}} \tag{36}$$

and

$$c''_{p,c}(\omega, 0) \equiv \Im\mathrm{m}[c_{p,c}^*(\omega, 0)] = c_p^0 \frac{\pi\tilde{\alpha}}{2\tilde{z}\tilde{\nu}} \left(\frac{\omega}{\omega_0}\right)^{-\frac{\tilde{\alpha}}{\tilde{z}\tilde{\nu}}} \tag{37}$$

Both real and imaginary parts show the same type of frequency dependence $c^{*}_{p,c}(\omega,0) \propto c''_{p,c}(\omega,0) \propto \omega^{-\frac{\tilde{\alpha}}{\tilde{z}\tilde{\nu}}}$ and diverge only at $\omega = 0$

Direct investigations of the frequency-dependent specific heat $c^{*}_{p}(\omega)$ in the vicinity of the critical point would be very interesting to prove the theoretical predictions given below. However, due to the small exponent $\tilde{\alpha}/\tilde{z}\tilde{\nu} = 0.056$, it may become very difficult to study the dynamical scaling behaviour of the frequency-dependent heat capacity near a second-order critical point by TMC. Those isothermal experiments must cover several frequency decades and have to be performed very close to the critical temperature. Therefore, one needs to put in a special effort in order to keep the temperature constant and to minimise the amplitude of the temperature modulations.

As expressed in Eq. (32), the frequency dependence of $c''_{p,c}(\omega)$ for $T = T_c$ resemble those for $(\alpha\lambda)_{T_c}$. From dynamic scaling arguments for the complex heat capacity, one gets for the ultrasonic attenuation per wavelength at the critical point [25] the following:

$$\alpha^{c}_{\lambda}(\omega) \equiv \alpha_{\lambda}(\omega,0) = \frac{\pi^2\tilde{\alpha}u_b^2g^2c_p^0}{2\tilde{z}\tilde{\nu}T_c c^2_{p,b}}\left(\frac{\omega}{\omega_0}\right)^{-\frac{\tilde{\alpha}}{\tilde{z}\tilde{\nu}}}, \tag{38}$$

where u_b is the non-critical contribution of the sound velocity. The frequency dependence of the critical absorption per wavelength and its critical slowing down is represented in Fig. 8 (see above).

For the attenuation α/f^2 at the critical point, Eq. (38) leads to a simple frequency dependence:

$$(\alpha/f^2)_{T_c} = Kf^{-[1+\tilde{\alpha}/(\tilde{z}\tilde{\nu})]} + B, \tag{39}$$

where B is a phenomenologically added background term, not further specified (Kirchhoff–Stokes law). In our case, B is identical to $(\alpha/f^2)_{b,c}$ at the critical point and K is a frequency-independent constant. The power-law behavior for $(\alpha\lambda)_{T_c}$ is expressed by the dashed line in Fig. 8 with a power of $-\tilde{\alpha}/(\tilde{z}\tilde{\nu}) = -0.056$.

In Fig. 11 the excess ultrasonic absorption $(\alpha/f^2)_{mix} = (\alpha/f^2) - (\alpha/f^2)_b$ (α/f^2 – observed attenuation of the mixture; $(\alpha/f^2)_b$ – background absorption calculated from the data of the pure components [29]) for a binary polymer mixture of polyethylene glycol and polypropylene glycol in the vicinity of the critical solution temperature ($T - T_c = 0.1$ K) is presented. Because α/f^2 shows only a weak temperature dependence close to T_c (see Eq. (34) and Fig. 8), it is appropriate to identify it as a measurement at the critical temperature. It can be seen, that the functional form of Eq. (39) is represented by the experimental data. Similar results have been found before for several binary mixtures of low molecular-weight components (e.g. [27,28]).

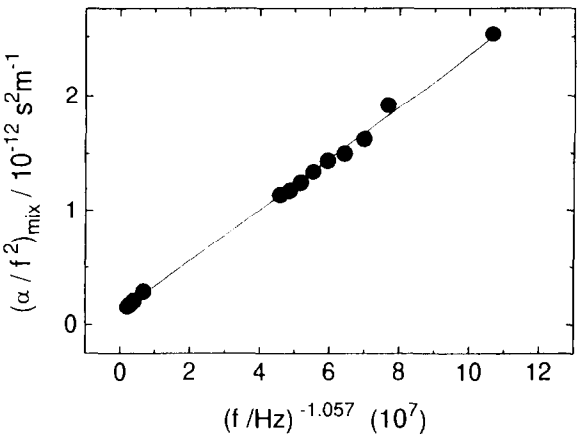

Fig. 11. $(\alpha/f^2)_{mix}$ as a function of $f^{-1.057}(\alpha/f^2)_{mix} = (\alpha/f^2)_b$, where α/f^2 is the observed attenuation of the mixture at $T = 28.9$°C and $(\alpha/f^2)_b$ is the background contribution to the observed attenuation calculated from the pure components [29].

To describe the critical ultrasound behavior in the whole frequency and temperature range, Bhattacharjee and Ferrell proposed a parameter-free relation for the reduced quantity $\alpha_\lambda/\alpha_{\lambda,c} = G_{BF}(\Omega)$, where α_λ is the contribution to the attenuation coefficient per wavelength from critical order parameter fluctuations at a given temperature and $\alpha_{\lambda,c}$ is the corresponding contribution at the critical temperature. The scaling function $G_{BF}(\Omega)$ only depends on the reduced frequency $\Omega = \omega/\omega_c$. Tanaka and Wada [26] have shown that the theories for critical ultrasonic absorption mentioned here can be brought to the following general functional form:

$$\alpha_\lambda(\omega,\varepsilon) \equiv 2\pi A'(\omega,\varepsilon)F(\Omega) = A(\omega,\varepsilon)F(\Omega). \tag{40}$$

They differ mainly in the functional form of the scaling function $F(\Omega)$. A' is an amplitude function which can be approximately expressed in all the

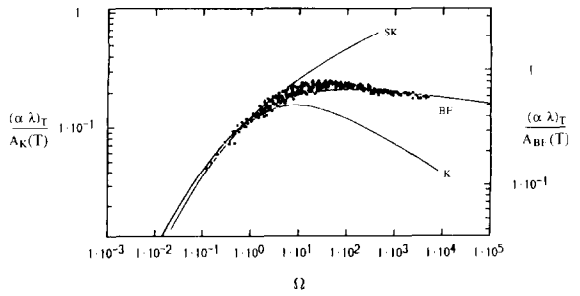

Fig. 12. Master plot of the reduced ultrasonic absorption per wavelength $(\alpha\lambda)_{T,crit.fl.}/A(T)$ (contribution from composition fluctuations) using the reduced frequency $\Omega = \omega/\omega_c$ (critical amplitude – $\omega_0 = 31$GHz; $\omega_c = \omega_0 \varepsilon^{\frac{\delta}{2\beta}}$) for an aniline/cyclohexane mixture with critical composition [28]. The solid curves are calculated using the Kawasaki (K,A_K), the Shiwa–Kawasaki (SK,A_K) and the Ferrell–Bhattacharjee (BK,A_{BF}) theory (see text).

theories, except for [25], by:

$$A'(\varepsilon) = \frac{u^2 g^2 c_p^0}{2T_c c_p^2} \varepsilon^{-\tilde{\alpha}/(\tilde{z}\tilde{\nu})} \tag{41}$$

In Fig. 12, the ratio $(\alpha\lambda)_{T,crit.fl.}/A(T)$ is plotted as a function of the reduced frequency $\Omega = \omega/\omega_c$ for an aniline/cyclochexane mixture with critical composition [28]. For comparison the calculated curves from the Kawasaki (K, A_K) [46], the Shiwa–Kawasaki (SK, A_K) [47] and the Ferrell–Bhattacharjee theory (BF, A_{BF}) [25] are plotted together with the experimental data. The explicit calculation of A would make it necessary to measure the heat capacity of the critical mixture in the vicinity of the critical point. Since no such data were available, the ultrasonic data are shifted together in order to obtain a master plot and A was used as a parameter to shift the theoretical curves to the experimental data. However, it appears that the experimental data are well represented by the Bhattacharejee–Ferrell scaling function. A similar result was recently found for a polymer mixture, where a more detailed comparison of the theories was carried out [29].

4. Concluding remarks

It was the aim of this paper to show the similar origin of sound absorption due to thermal relaxation processes in longitudinal ultrasonic experiments and the frequency-dependent complex heat capacity measured in temperature-modulated calorimetric (TMC) experiments.

The theories for the ultrasonic attenuation near a second-order critical point, which include the description of the complex frequency-dependent heat capacity, are referred to and illustrated with some examples. For experiments in the vicinity of a critical point, the ultrasonic spectroscopy can be considered as a high-frequency extension of the TMC. However, no such direct frequency-dependent heat capacity measurements are known until now. For a better understanding of the dynamic glass transition, combined longitudinal and shear ultrasonic measurements together with TMC would also be of interest.

From the foregoing considerations, especially from the requirements of the theories, the problems for a further development of TMC or TMDSC can be summarised as follows:

(i) The amplitudes of the temperature variations need to be minimised ($\delta T \rightarrow 0$) in order to fulfill the requirements of the linear response theory and to prevent irreversible changes in the samples or slow kinetic effects (e.g. crystallisation and melting in polymers).

(ii) The signal-to-noise ratio must be considerably increased, especially for high accuracy isothermal frequency-depended heat capacity measurements.

(iii) The frequency range of the method must be considerably extended, e.g. by a combination of different techniques.

However, it seems rather difficult to fulfill the requirements, especially for high-accuracy isothermal frequency-dependent heat capacity measurements over a broad frequency range by a simple modification of the existing DSC equipment. For those measurements a special design (e.g. a modified specific heat spectroscopy) seems to be necessary.

Another important problem that has to be solved is the understanding of the frequency-dependent heat capacity in heterogeneous systems, where the heat conductivity between the components has to be taken into consideration.

Acknowledgements

The financial support of the Deutsche Forschungsgemeinschaft (Grant: Al 93/1-2) and the Forschungs-

gemeinschaft Kunststoffe e.V. is gratefully acknowledged. The author wishes to thank Dr. W. Mayer, Dr. J. Schawe, Prof. C. Schick and Prof. D. Woermann for the stimulating discussions and the experimental material. Furthermore, the author thanks Dipl.-Chem. E. Bittmann and Dip.-Phys. S. Hoffmann for performing the ultrasonic measurements on the aniline/cyclohexane and the PEG/PPG mixtures.

References

[1] M. Reading, D. Elliot and V.L. Hill, J. Thermal Anal., 40 (1993) 949.
[2] P.S. Gill, S.R. Sauerbrunn and M. Reading, J. Thermal Anal., 40 (1993) 931.
[3] M. Reading, Trends in Polymer Sci., 8 (1993) 248.
[4] M. Reading, B. Hahn, B. Crowe, US Patent, 5,224,775.
[5] B. Wunderlich, Y. Yin and A. Boller, Thermochim. Acta, 238 (1994) 277.
[6] J.E.K. Schawe, Thermochim. Acta, 261 (1995) 183.
[7] J.E.K. Schawe, Thermochim. Acta, 260 (1995) 1.
[8] A. Hensel, J. Dobbertin, J.E.K. Schawe, A. Boller and C. Schick, J. Thermal. Anal, 46 (199..) 935.
[9] N.O. Birge and S.R. Nagel, Phys. Rev. Letters, 25 (1985) 2674.
[10] N.O. Birge and S.R. Nagel, Phys. Rev. Sci. Instr., 58 (1987) 1464.
[11] Y.H. Jeong, personal communication.
[12] E. Gmelin, J. Thermochim. Acta(this issue).
[13] O.M. Corbino, Phys. Z, 12 (1911) 292; ibid. Phys. Z. 10 (1910) 413.
[14] J. Fourier, Mémoires de l'Académie des sciences, 4(1824)185; ibid Mémoires del'Académie des sciences 5 (1826) 153–246.
[15] M.A.J. Angström Phil. Mag. 25 (1863).
[16] G. Busse, NDT and E International, 27 (1994) 253.
[17] A. Hammiche, M. Reading, H.M. Pollock, M. Song and D.J. Hurston, Rev. Sci. Instr. 67 (1996) (in press).
[18] P.S. Laplace, Ann. Chim. Phys. Tomme iii (1816) 238.
[19] K.F. Herzfeld and F.O. Rice, Phys. Rev., 31 (1928) 691.
[20] K.F. Herzfeld and T.A. Litowitz, Absorption and Dispersion of Ultrasonic Waves, Academic, New York, 1959.
[21] L.D. Landau and E.M. Khalatnikov, Collected Papers of L.D. Landau, D. Ter Haar (Ed.), New York, 1965, p. 626; Dokl. Akad. Nauk SSSR 96 (1954) 469.
[22] I. Mandelstam and M. Leontovich, Compt. Rend. Acad. Sci. U.R.S.S., 3 (1936) 111; Zhur. Eksp. i Teoret. Fiz., 7(1938) 438.
[23] M. Fixman, J. Chem. Phys., 36 (1962) 1961.
[24] L. Mistura, J. Chem. Phys., 57 (1972) 2311; L. Mistura, Proceedings of the Varenna Summer School on Critical Phenomena, Acedemic, New York, 1971.
[25] J.K. Bhattacharjee and R.A. Ferrell, Phys. Rev., A 24 (1981) 1643; R.A. Ferrell and J.K. Bhattacharjee, ibid., A 31 (1985) 1788.
[26] H. Tanaka and Y. Wada, Phys. Rev., A 32 (1985) 512.
[27] C. Bakken, L. Belkoura, S. Fusenig, T. Müller-Kirschbaum and D. Woermann, Ber. Bunsenges. Phys. Chem., 94 (1991) 150.
[28] E. Bittmann, I. Alig and D. Woermann, Ber. Bunsenges. Phys. Chem., 98 (1994) 189.
[29] W. Mayer, S. Hoffmann, G. Meier and I. Alig, Phys. Rev., E 55 (1997) 3102.
[30] J. Meixner, Ann. Physik [5] 43 (1943) 470; Z. Naturforscher 4a (1949) 594; 9a (1954) 654; Acustica 2 (1952) 101; Kolloid-Z. 134 (1953) 3.
[31] N.O. Birge, Phys. Rev., B34 (1986) 1631.
[32] R. Kohlrausch, Pogg. Ann. Phys., 91 (1854) 179.
[33] H. Vogel, Phys. Z., 22 (1921) 645; G.S. Fulcher, J. Am. Ceram. Soc., 8 (1923) 339.
[34] L.D. Landau and E.M. Lifschitz, Statistiche Pysik, Band 1, Akademie-Verlag, Berlin, 1978.
[35] E.-J. Donth, Glasübergang, Academie-Verlag, Berlin, 1980.
[36] W. Götze and L. Sjörgren, Transp. Theory Stat. Phys., 24 (1995) 801.
[37] K.L. Ngai, Comments Solid State Phys., 9 (1979) 121.
[38] L.D. Landau and E. M. Lifshitz, Fluid Mechanics, J.B. Sykes and W. H. Reid, Pergamon, London, 1959, translation.
[39] M. Schulz and I. Alig, J. Chem. Phys., 97 (1992) 2772.
[40] I. Alig, F. Stieber and S. Wartewig, Polymer, 32 (1991) 2146; J. Non-Cryst. Solids, 131–132 (1991) 808.
[41] C.W. Garland and G.J. Sanchez, J. Chem. Phys., 79 (1983) 3090; ibid. 79 (1983) 3100.
[42] D. Woermann, Progr. Colloid Polym. Sci., 84 (1991) 165.
[43] L.A. Zubkov, Yu.S. Manucharov, S.A. Manucharova and R.K. Turniyasov, Vysokomol. Soed., A29 (1987) 1932.
[44] D.B. Fenner, J. Chem. Phys., 87 (1987) 2377.
[45] U. Kaatze and U. Schreiber, Chem. Phys. Lett., 148 (1988) 241.
[46] K. Kawasaki, Phys. Rev., A1 (1970) 1750.
[47] (a) Y. Shiwa and K. Kawasaki, Prog. Theor. Phys., 66 (1981) 118; (b) Y. Shiwa and K. Kawasaki, Prog. Theor. Phys., 66 (1981) 406.
[48] D.M. Ruhland and Kroll, Phys. Rev., A 23 (1989) 371.
[49] B. Knecht and D. Woermann, Z. Phys. Chem., 191 (1995) 265.